7-21-2016

Accuracy and precision of quantitative 31P-MRS measurements of human skeletal muscle mitochondrial function

Gwenael Layec

J. R. Gifford

Joel D. Trinity

Corey R. Hart

Ryan S. Garten

See next page for additional authors

Authors

Gwenael Layec, J. R. Gifford, Joel D. Trinity, Corey R. Hart, Ryan S. Garten, Song-young Park, Yann Le Fur, Eun-Kee Jeong, and Russell S. Richardson

Accuracy and precision of quantitative ^{31}P-MRS measurements of human skeletal muscle mitochondrial function

Gwenael Layec,[1,2] Jayson R. Gifford,[2,3] Joel D. Trinity,[1,2] Corey R. Hart,[2,3] Ryan S. Garten,[1,2] Song Y. Park,[2,3] Yann Le Fur,[5] Eun-Kee Jeong,[4] and Russell S. Richardson[1,2,3]

[1]*Department of Medicine, Division of Geriatrics, University of Utah, Salt Lake City, Utah;*
[2]*Geriatric Research, Education, and Clinical Center, George E. Whalen Veterans Affairs Medical Center, Salt Lake City, Utah;*
[3]*Department of Exercise and Sport Science, University of Utah, Salt Lake City, Utah;*
[4]*Department of Radiology and Utah Center for Advanced Imaging Research, University of Utah, Salt Lake City, Utah; and*
[5]*Aix-Marseille Université, Centre national de la recherche scientifique, Center for Magnetic Resonance in Biology and Medicine,Unité Mixte de Recherche 7339, Marseille, France*

Layec G, Gifford JR, Trinity JD, Hart CR, Garten RS, Park SY, Le Fur Y, Jeong EK, Richardson RS. Accuracy and precision of quantitative ^{31}P-MRS measurements of human skeletal muscle mitochondrial function. *Am J Physiol Endocrinol Metab* 311: E358 –E366, 2016. First published June 14, 2016; doi:10.1152/ajpendo.00028.2016.

Although theoretically sound, the accuracy and precision of ^{31}P- magnetic resonance spectroscopy (^{31}P-MRS) approaches to quantitatively estimate mitochondrial capacity are not well documented. Therefore, employing four differing models of respiratory control [linear, kinetic, and multipoint adenosine diphosphate (ADP) and phosphorylation potential], this study sought to determine the accuracy and precision of ^{31}P-MRS assessments of peak mitochondrial adenosine-triphosphate (ATP) synthesis rate utilizing directly measured peak respiration (State 3) in permeabilized skeletal muscle fibers. In 23 subjects of different fitness levels, ^{31}P-MRS during a 24-s maximal isometric knee extension and high-resolution respirometry in muscle fibers from the vastus lateralis was performed. Although significantly correlated with State 3 respiration (r = 0.72), both the linear (45 + 13 mM/min) and phosphorylation potential (47 + 16 mM/min) models grossly overestimated the calculated in vitro peak ATP

synthesis rate ($P < 0.05$). Of the ADP models, the kinetic model was well correlated with State 3 respiration ($r = 0.72$, $P < 0.05$), but moderately overestimated ATP synthesis rate ($P < 0.05$), while the multipoint model, although being somewhat less well correlated with State 3 respiration ($r = 0.55$, $P < 0.05$), most accurately reflected peak ATP synthesis rate. Of note, the PCr recovery time constant (r), a qualitative index of mitochondrial capacity, exhibited the strongest correlation with State 3 respiration ($r = 0.80$, $P < 0.05$). Therefore, this study reveals that each of the ^{31}P-MRS data analyses, including PCr r, exhibit precision in terms of mitochondrial capacity. As only the multipoint ADP model did not overstimate the peak skeletal muscle mitochondrial ATP synthesis, the multipoint ADP model is the only quantitative approach to exhibit both accuracy and precision.

Keywords: mitochondrial capacity assessment; State 3 respiration; respirometry; PCr recovery

AS THE ATP GENERATED DURING RECOVERY from exercise is driven almost exclusively by oxidative metabolism (6, 51), the rate of phosphocreatine (PCr) recovery is commonly used as an indicator of skeletal muscle mitochondrial phosphorylation “capacity” or function (19, 59). Given the mono-exponential behavior of PCr kinetics postexercise (41), a common approach has been to utilize PCr r or the rate constant (k) to qualitatively assess muscle mitochondrial function (43). Quantitative approaches relying on models of respiratory control have also been pro- posed to estimate mitochondrial capacity in vivo. For instance, kinetic models of respiratory control by the phosphorylation potential (ADP·Pi/ATP, the Kinetic Phosphorylation Potential model) (66) or ADP (4, 17) (the Kinetic ADP model), have been used to estimate the peak rate of mitochondrial ATP synthesis (V_{max}). To improve the accuracy of this estimate, a refinement of the latter approach using a multipoint analysis of the recovery (the Multipoint ADP model) has also been pro- posed (21). An additional, frequently used method is based on the central role played by the creatine kinase reaction in the intracellular communication between the sites of ATP demand and synthesis (the Linear

model) (21), and is derived from the electrical analog model of respiratory control (43). However, the accuracy and precision of these quantitative approaches of estimating mitochondrial capacity compared with the direct measurement of mitochondrial functional capacity is uncommon.

This not well-validated array of ^{31}P-MRS data analysis approaches to assess mitochondrial function in vivo complicates comparisons between studies and, as they can lead to different conclusions, may call into question the generalization of ^{31}P-MRS results (33). Therefore to appropriately facilitate the widespread use of ^{31}P-MRS, it is critical to evaluate the relationship between each model of respiratory control and intrinsic mitochondrial respiration capacity, measured in vitro, to clarify whether one approach is preferable to the others. Interestingly, some validation with in vitro techniques has been performed for these ^{31}P-MRS-based approaches (5, 28, 32, 42). However, these comparisons were likely somewhat affected by the fact that ^{31}P-MRS provides a physiologically relevant functional assessment of muscle mitochondrial properties within the environment of the muscle, whereas enzymatic activities measure the maximal flux at specific points along the metabolic pathway. Thus, the latter, may not accurately reflect maximal oxidative phosphorylation flux in skeletal muscle (2). Similarly, respiration measurements in isolated mitochondria, although providing a more direct measurement, may be affected by the biased selection of a particular mitochondrial population and the disruption of mitochondrial interactions during the isolation procedure, which in turn can alter mitochondrial function (26, 50). However, this issue appears to have been overcome by the development of the in vitro permeabilized fiber technique, which seems to preserve most of the functional properties of the skeletal muscle mitochondria (26, 50).

Therefore, the purpose of this study, employing comprehensive in vivo and in vitro analyses, was to determine the accuracy and precision of the peak mitochondrial ATP synthesis rates of four models of respiratory control (linear, kinetic, and multipoint ADP, and phosphorylation potential) against State 3 respiration directly assessed in permeabilized skeletal muscle fibers. We hypothesized that all the ^{31}P-MRS data analysis approaches would be significantly correlated with State 3 respiration assessed in vitro. However, on the basis of previous studies (19, 27, 33), we hypothesized that

the peak ATP synthesis rates estimated with the linear and phosphorylation potential models would overestimate those calculated from State 3 respiration in vitro.

METHODS

Subjects. Following informed consent procedures, 23 (20 males, 3 females) subjects, exhibiting a variety of physical activity levels, participated in this study (Table 1). All subjects were nonsmokers, free of diabetes and known cardiovascular, peripheral vascular, neuromuscular, or pulmonary disease. Additionally, none of the subjects were taking medications known to affect muscle function. The women, who were all premenopausal, were studied in the MR scanner during days 1–7 of their menstrual cycle to standardize the influence of female hormones. The study was approved by the Institutional Review Boards of both the University of Utah and the Salt Lake City Veterans Affairs Medical Center.

Exercise protocol. On the first day, participants were familiarized with testing procedures and performed preliminary assessments. On a separate day, subjects performed the isometric knee extension exercise in the whole body MRI system (TimTrio 2.9T; Siemens Medical Systems, Erlangen, Germany). While positioned supine, the knee of the dominant leg was fixed at ~135° over a custom-built apparatus, and the foot was attached to a strain gauge (SSM-AJ-250; Interface, Scottsdale, AZ). To minimize hip movement and back extension during the contraction, participants were secured to the bed with nonelastic straps placed over the hips and the thigh of the leg being interrogated. The force signal was collected with a sample frequency of 100 Hz, converted from analog-to-digital (MP150, Biopac Systems), and recorded on a personal computer (Acknowledge, Biopac Systems). Each participant performed two baseline/practice maximum voluntary contractions (MVC) of ~5–10 s duration with 1 min of recovery between each. After ~10 min of rest and 4 min of baseline data collection, subjects performed a maximal voluntary isometric contraction for 24 s followed by 5 min of recovery. Based on preliminary testing, this protocol was designed to elicit a substantial depletion in PCr content without inducing acidosis, as this is known to complicate the interpretation of the PCr recovery kinetics. On a separate day, a percutaneous biopsy of the vastus lateralis muscle ~3.5 cm deep, 15 cm proximal to

the knee and slightly distal to the ventral mid-line of the muscle was obtained from the same leg. The 5-mm diameter biopsy needle (Bergström) was attached to sterile tubing and a syringe to apply a negative pressure to assist in the muscle sample collection (12). Immediately after the muscle sample (~100 mg) was removed from the leg, a portion of the sample (~20 mg) was immersed in ice-cold biopsy preservation fluid (BIOPS) for respiratory analysis (47) (in mM: 2.77 CaK^2EGTA, 7.23 K_2EGTA, 20 imidazole, 50 K^+MES, 20 taurine, 0.5 dithiothreitol, 6.56 MgCl2, 5.77 ATP, 15 PCr, pH 7.1). Visits were separated by at least 7 days to ensure adequate healing from the biopsy procedure or enough recovery from the exercise. All experimental trials were performed in a thermoneutral environment (~20°C) and following an overnight fast.

Table 1. *Subject characteristics*

Characteristics		
Anthropometric characteristics		
Age, yr		25±4
Height, cm		169±37
Weight, kg		73±12
BMI, kg/m^2		24±4
Functional characteristics		
Steps per day		8,459± 2,764
Moderate to vigorous activity, min/day		51±19
Blood and plasma characteristics		
Glucose, mg/dl		79±11
Cholesterol, mg/dl		170±24
Triglycerides, mg/dl		99±35
HDL, mg/dl		55±13
LDL, mg/dl		104±21
WBC, K/µl		5.4±1.0
RBC, M/µl		5.2±0.4
Hemoglobin, g/dl		15.6±1.1
Hematocrit, %		45±3
Neutrophil, K/µl		2.9±0.9
Lymphocyte, K/µl		2.0±0.7
Monocyte, K/µl		0.4±0.1

Values are expressed as means + SD; *n* = 23. Body mass index, BMI; high-density lipoprotein, HDL; low-density lipoprotein, LDL; white blood cells, WBC; red blood cells, RBC.

31P-MRS. MRS was performed using a clinical 2.9T MRI system (Tim-Trio; Siemens Medical Solutions, Erlangen, Germany) operating at 49.9 MHz for ^{31}P

resonance. ^{31}P-MRS data were acquired with a ^{31}P-proton (^{1}H) dual-surface coil with linear polarization (Rapid Biomedical, Rimpar, Germany) positioned above the quadriceps. The ^{31}P single-loop coil diameter was 125 mm, which surrounded the 110-mm ^{1}H coil loop. After a three-plane scout proton image, advanced localized volume shimming was performed. Before each experiment, two fully relaxed ^{31}P-MRS spectra were acquired at rest with three averages per spectrum and a repetition time (TR) of 30 s. Then, ^{31}P-MRS data acquisition was performed throughout the rest- exercise-recovery protocol using an FID (free-induction-decay) pulse sequence with a 2.56 ms adiabatic half-passage excitation RF (radio frequency) pulse and the following parameters (TR = 2 s, receiver bandwidth = 5 kHz, 1,024 data points, and 3 averages per spectrum). Saturation factors were quantified by the comparison between fully relaxed (TR = 30 s) and partially relaxed (TR = 2s) spectra.

Relative concentrations of phosphocreatine [PCr], inorganic phosphate [Pi], phosphodiester (PDE), and [ATP] were obtained by a time domain-fitting routine using the AMARES algorithm (64) incorpo- rated into the CSIAPO software (38). Intracellular pH was calculated from the chemical shift difference between the Pi and PCr signals (58). The free cytosolic [ADP] was calculated from [PCr] and pH using the creatine kinase (CK) equilibrium constant (K_{CK} = 1.66 X 10^{9} M^{-1}) and the assumption that PCr represents 85% of the total creatine content (16). The resting concentrations were calculated from the average peak areas of the two relaxed spectra (TR = 30 s; n = 3) recorded at rest and assuming an 8.2 mM [ATP] under these conditions.

31P-MRS data analysis. PCr recovery kinetics was determined by fitting the PCr time-dependent changes during the recovery period to a single exponential curve described by the following equation:

$$[PCr]\,(t) = [PCr]_{end} + [PCr]_{cons}(1 - e^{-(t/r)})$$

where $[PCr]_{end}$ is the concentration of [PCr] measured at end of exercise and $[PCr]_{cons}$ refers to the amount of PCr consumed at the end of the exercise session, and r reflects the time constant of the recovery, a relative measure of muscle oxidative capacity (21, 42– 44). The initial rate of PCr resynthesis (Vi) was calculated as follows:

$$Vi = k \times [PCr]_{cons}$$

in which $[PCr]_{cons}$ represents the amount of PCr consumed at the end of exercise and the rate constant, $k = 1/r$.

On the basis of the assumption that in the absence of an oxygen limitation and changes in mitochondrial redox balance, phosphate potential ([Pi] X [ADP]/[ATP]) controls the rate of oxidative phosphorylation with a K_m of 0.11 (66), we calculated $V_{max\ pp}$ (kinetic phosphorylation potential model) as follows:

$$V_{max\ pp} = Vi\ (1 + [K_m / ([Pi]_{end} \times [ADP]_{end} / [ATP])])$$

Based on the sigmoid relationship between the oxidative ATP production rate and free cytosolic ADP concentration (kinetic ADP model), $V_{max\ ADP}$ (in mM/min) was calculated using the initial rate of PCr synthesis during the recovery period and [ADP] obtained at the end of exercise as previously described (60):

$$V_{max\ ADP} = Vi\ [1 + (K_m / [ADP]_{end})^{2.2}]$$

By use of multipoint analysis (21, 35), the control of respiration rate by ADP was fitted using nonlinear least square techniques from the following function (multiple-point ADP model) (67):

$$Vi = (V_{max\ mp} \times [ADP]^{nH}) / (K_m^{nh} + [ADP]^{nh})$$

in which n_H is the Hill coefficient, K_m is the ADP value at half- maximal Vi, and $V_{max\ mp}$ is the maximal ADP-stimulated respiration rate. Although we acknowledge that even in absence of ADP there is some mitochondrial respiration (uncoupled respiration), the minimal ADP-stimulated respiration rate (V_{min}) was not included in the model, as the estimation of this parameter has poor accuracy due to the low signal-to-noise ratio of the respiration rate and [ADP] in the resting state.

According to the linear model of oxidative phosphorylation de- scribed by Meyer (43), the theoretical peak rate of oxidative phosphorylation can be estimated as the product of k_{PCr} and resting [PCr] using the following equation (linear model) (21):

$$V_{max\ lin} = k \times PCr_{rest}$$

Model variables were determined with an iterative process by minimizing the sum of squared residuals (RSS) between the fitted function and the observed values. Goodness of fit was assessed by visual inspection of the residual plot and the frequency plot distribu- tion of the residuals, x^2 values and the coefficient of determination (r^2)

calculated as follows:

$$r^2 = 1 - (SS_{reg}/SS_{tot})$$

with SS_{reg} representing the sum of squares of the residuals from the fit and SS_{tot} being the sum of squares of the residuals from the mean.

Mitochondrial respiration. Muscle samples were prepared and permeabilized for mitochondrial respiration analysis as previously described (47). Briefly, BIOPS-immersed fibers were carefully separated with fine-tip forceps and subsequently bathed in a BIOPS-based saponin solution (50 µg saponin/ml BIOPS) for 30 min. Following saponin treatment, muscle fibers were rinsed twice in ice-cold mitochondrial respiration fluid (MIR05, in mM: 110 sucrose, 0.5 EGTA, 3 $MgCl_2$, 60 K-lactobionate, 20 taurine, 10 KH_2PO_4, and 20 HEPES, and BSA 1 g/l, pH 7.1) for 10 min each rinse. After the muscle sample was gently dabbed with a paper towel to remove excess fluid, the wet weight of the sample was measured using a standard calibrated scale (2– 4 mg). The muscle fibers were then placed in the respiration chamber (Oxytherm, Hansatech Instruments, UK) in 2 ml of MIR05 solution and warmed to 37°C. MIR05 was air saturated with O_2 concentrations of ~190 to ~175 µM O_2 from the start to finish of the experiments. After allowing the muscle 10 min to equilibrate, mitochondrial respiratory function was assessed in duplicate. State 2 respiration was measured after the addition of malate (2 mM), and glutamate (10 mM) in saturating concentrations. State 3 respiration with electron flux through CI was measured after the addition of ADP (5 mM), and maximal coupled respiration (State 3) with convergent electron flux through CI + CII was achieved by adding saturating concentrations of succinate (10 mM) to the respiration chamber. This combination of substrates was chosen to reconstitute the operation of the tricarboxylic acid cycle and prevent the depletion of key metabolites from the mitochondrial matrix, thus providing suitable conditions for evaluating maximal physiological oxidative phosphorylation capacity (7). Then, cytochrome *c* (10 µM) was added to test for outer mitochondrial membrane integrity. Only samples demonstrating intact mitochondrial membrane integrity (<10% increase in respiration in response to cytochrome *c*) were included in this analysis. Assuming a P/O ratio of 2.47 (3) and muscle density of 1.049 kg/l, the maximal ADP-stimulated respiration was converted into ATP synthesis rate ($mM \cdot min^{-1} \cdot l^{-1}$) to assess the accuracy of the quantitative ^{31}P-

MRS data analysis approaches.

Thigh volume. Thigh volume and quadriceps muscle mass were calculated based on thigh leg circumference (3 sites: distal, middle, and proximal), thigh length, and skinfold measurements (18), a method that has demonstrated excellent agreement with thigh volume assessed with ^{1}H-MR imaging.

Physical activity level. Both a subjective modified physical activity level (PAL) recall questionnaire and objective accelerometer data were used to assess physical activity. The PAL questionnaire included items regarding the average type, frequency, intensity, and duration of physical activity in any given week. After receiving standardized operating instructions, subjects wore the accelerometer (GT1M; Actigraph, Pensacola, FL) for 7 continuous days, with adherence automatically assessed by the data output. Average daily physical activity was expressed as steps per day and the time spent in moderate to vigorous physical activity. Based on the recommendations of the manufacturer of the accelerometer, thresholds for sedentary, light, and moderate to vigorous activity were defined as <99, 100-1,959, and 1,952+ counts/min, respectively.

Statistical analysis. The assessment of differences between base- line and exercise was performed with either paired *t*-tests or nonparametric Wilcoxon tests, where appropriate (Statsoft, version 5.5; Statistica, Tulsa, Oklahoma). Potential relationships between variables were assessed using Pearson's correlation analysis or the nonparametric Spearman rank order correlation. Statistical significance was accepted at $P < 0.05$. Results are presented as means + SD in tables and means + SE in the figures for clarity.

RESULTS

High-energy phosphate compounds, intracellular pH, and mitochondrial function in vivo. Intracellular metabolite concentrations and pH at rest and at the end of the exercise are summarized in Table 2. Unlike pH, which was not significantly different from baseline after exercise ($P > 0.05$), PCr was significantly decreased ($P < 0.01$), and both Pi and ADP were significantly increased compared with baseline ($P < 0.01$).

Typical examples of the PCr dynamics during the recovery period as well as the

relationship between PCr resynthesis rate and ADP in a representative subject are displayed in Fig. 1. The mean PCr r and kinetic parameters estimated with the multiple-point ADP model are presented in Table 2. V_{max} from the linear and phosphorylation potential models were significantly higher than V_{max} from the kinetic and multiple-point ADP models ($P < 0.05$; Fig. 2). In addition, the peak ATP synthesis rates from the linear, phosphorylation potential, and ADP kinetic models were significantly higher than the ATP synthesis rate calculated from State 3 CI + CII in vitro ($P < 0.05$; Fig. 2).

Table 2. *Muscle metabolites and pH at rest and in response to knee-extensor exercise, and parameters of mitochondrial function measured by ^{31}P-MRS*

Concentrations	Resting	End Exercise	*P*
	Means SD	Means SD	
	31±4	16±5	*
Pi, mM	1±0.6	11±3	*
ADP, μM	8±1	64±26	*
PCr recovery kinetics and mitochondrial function			
Time constant, s	44±11		
V_{max} ADP multipoint, mM/min	20±5		
K_m, μM	25±6		
Hill coefficient	2.6±0.8		

Values expressed as means + SD. PCr, phosphocreatine; Pi, inorganic phosphate; ADP, adenosine diphosphate; PDE, phosphodiester; K_m, ADP value at half-maximal oxidative ATP synthesis rate. *$P <$ 0.01, significantly different from baseline.

Respiration in permeabilized fibers and relationship with in vivo measurements. State 2 respiration was 16.5 + 10.2 $pM \cdot s^{-1} \cdot mg^{-1}$ wet wt and reached 45.6 + 12.6 $pM \cdot s^{-1} \cdot mg^{-1}$ wet wt during State 3 respiration due to convergent electron flux through Complex I and II. As illustrated in Fig. 3, State 3 CI + CII was significantly correlated with PCr r ($r = 0.8$, $P < 0.05$; Fig. 3*A*) and V_{max} from all four models ($r = 0.55–0.72$, $P < 0.05$; Fig. 3, *B*–*E*).

DISCUSSION

This study, employing comprehensive in vivo and in vitro metabolic analyses, sought to determine the accuracy and precision of the peak mitochondrial ATP synthesis rates of four models of respiratory control (linear, kinetic, and multipoint ADP and phosphorylation potential). Consistent with our first hypothesis, in terms of precision, V_{max}

calculated from each of the quantitative models of respiratory control correlated with the State 3 respiration in vitro (r = 0.55 to 0.72). Although not the primary aim of the study, the PCr r, a qualitative index of mitochondrial capacity, exhibited the strongest association with State 3 respiration in vitro (r = 0.80). However, in terms of accuracy, the peak ATP synthesis rates from the linear, phosphorylation potential, and ADP kinetic models were significantly higher than the ATP synthesis rate calculated from the State 3 respiration in vitro. Therefore, this study reveals that each of the ^{31}P-MRS data analysis approaches, including the PCr r, provides evidence of being precise. However, only the multipoint ADP model did not overstimate the peak rate of skeletal muscle mitochondrial ATP synthesis, supportive of the conclusion that this is the only quantitative model exhibiting both accuracy and precision.

Accuracy and precision of ^{31}P-MRS mitochondrial function measurements. An important finding of this study was that the State 3 respiration with convergent electron flux through CI and CII in permeabilized fibers from the vastus lateralis muscle correlated significantly, although to somewhat differing degrees, with all four of the quantitative ^{31}P-MRS approaches *to* assess mitochondrial phosphorylation capacity in the quadriceps of the same cohort of subjects (r = 0.55 to 0.72; Fig. 3). In addition, although not the primary aim of the study, we observed that the PCr r, a qualitative index of mitochondrial capacity, demonstrated a strong correlation with State 3 respiration (r = 0.80, P < 0.05). Consistent with our results, some of these ^{31}P-MRS indexes of mitochondrial capacity have previously been documented to correlate with in vitro markers of mitochondrial content or function (5, 28, 32, 42). In accord with the current findings (Fig. 3*E*), the peak rate of mitochondrial ATP synthesis from the linear model has previously been correlated with State 3, CI and CII respiration in both isolated mitochondriafrom young adults (r = 0.71) (28) and permeabilized fibers from older individuals (r = 0.69)(5). Furthermore, citrate synthase activity (r = 0.63 to 0.64), a marker of mitochondrial content (31), demonstrated a good agreement with the peak rate of mitochondrial ATP synthesis from the kinetic ADP model (r = 0.64) in the calf muscle of young adults (32). In addition, an extensive review of the literature recently confirmed the consistency of the ADP kinetics model with direct invasive measurements of muscle O_2 consumption using a common analytical framework (19).

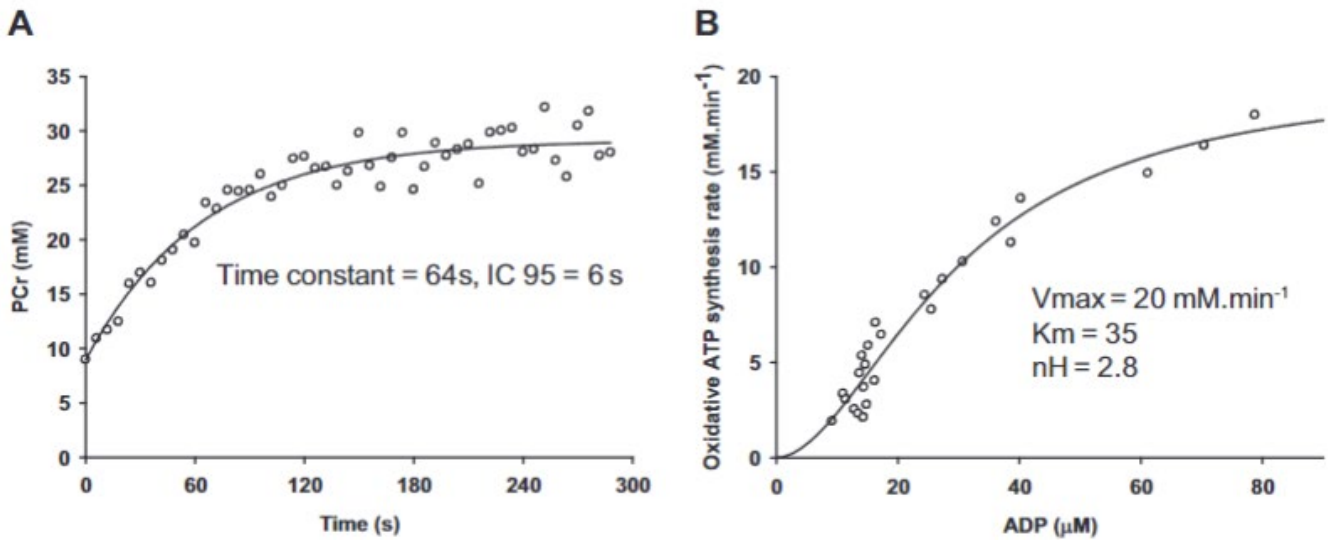

Fig. 1. Typical example of postexercise [PCr] resynthesis with respect to time, fitted according to a monoexponential function (*A*) and the corresponding PCr resynthesis rate (mM/min) with respect to ADP concentration, a key regulator of mitochondrial respiration, fitted according to a sigmoid function (*B*). IC 95, 95% confidence interval of the time constant; *nH*, Hill coefficient; and K_m, ADP value at half-maximal oxidative ATP synthesis rate.

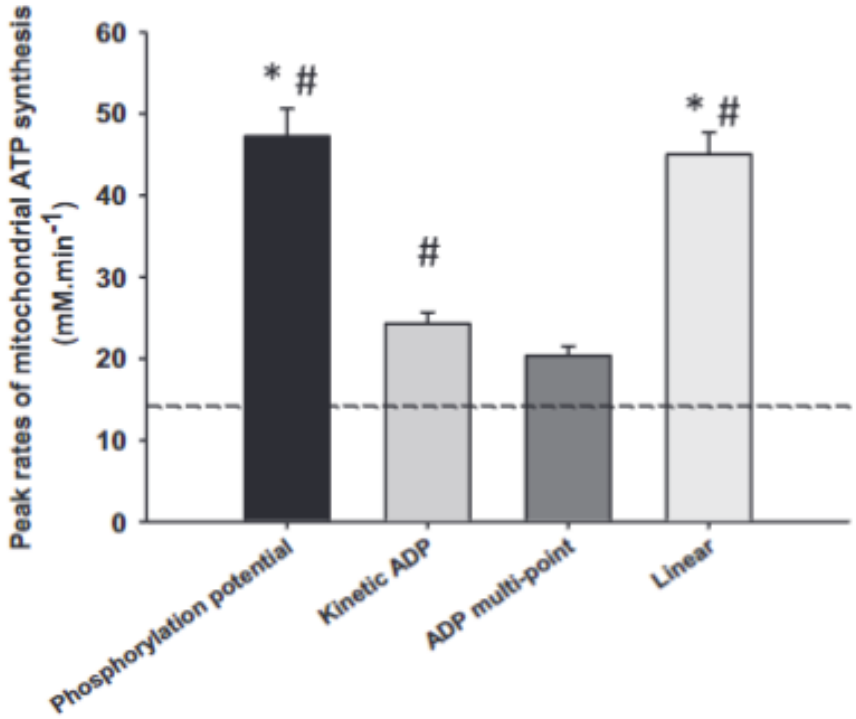

Fig. 2. Peak rates of mitochondrial ATP synthesis based on respiratory control models by the phosphorylation potential (kinetic phosphorylation potential model), ADP using two parameters (kinetic ADP model) or a multipoint analysis (multiple-point ADP model), and the electrical analog model of respiratory (linear model). Dashed line, peak rate of mitochondrial ATP synthesis estimated from the maximal ADP-stimulated respiration in vitro assuming a P/O ratio of 2.47. *P < 0.05, significantly different from ADP models; #P < 0.05, significantly different from calculated in vitro value.

Previous investigations have documented that the r/rate constant of PCr recovery kinetics exhibit moderate to good agreement (r = 0.48 to 0.84) with citrate synthase activity in the human calf (32, 42) and rat gastrocnemius muscles (44). In addition, the injection of a CI inhibitor elicited a parallel decrease in the PCr recovery rate constant measured by ^{31}P-MRS and the State 3 respiration from CI in isolated mitochondria from the tibialis anterior of rats (62). Therefore, taken together, these findings strongly support the use of ^{31}P-MRS to assess the functional properties of skeletal muscle mitochondria in vivo.

It is interesting to note that the correlation coefficients observed in the current study between the in vitro and in vivo measurements of mitochondrial function appear to be slightly higher than the values reported in previous studies (28, 32, 42). This apparently better agreement may originate from the permeabilized fiber technique

employed in the current study to assess the mitochondrial properties in vitro. Indeed, it has been advocated that the permeabilized fiber approach enables the assessment of all cellular populations of mitochondria and preserves the integrity of the mitochondria, thus providing a more physiological measurement of mitochondrial respiration (26, 50). Interestingly, although used as an external control in this study, by means of construct validity, the high level of agreement between the in vivo measurements of mitochondrial function and the assessment of mitochondrial respiratory capacity in permeabilized fibers lends further credence to this technique.

Of note, the r/rate constant of PCr recovery kinetics and the kinetic ADP model have previously exhibited good agreement with citrate synthase activity, but not with cytochrome *c* oxidase activity (32). However, it should be acknowledged that the maximal flux at specific points of the metabolic pathway does not necessarily accurately reflect the maximal oxidative phosphorylation flux (2). Specifically, it is unclear whether cytochrome *c* oxidase, which is the terminal complex of the mitochondrial electron transport chain, is an appropriate mitochondrial biomarker, as the flux through the electron transport chain is usually in excess relative to the maximal flux through ATP synthase (7). Also, while citrate synthase activity closely reflects mitochondrial content in the skeletal muscle of healthy adults (31), the muscle respiratory capacity normalized for mitochondrial content can vary substantially between healthy individuals with different activity levels (15). Therefore, based on these considerations regarding the use of mitochondrial enzyme activity to assess metabolic capacity, this approach may not fully reflect the functional capacity of the mitochondria, or at least not as closely as the State 3, complex I and II respiration in permeabilized fibers, as employed in the current study.

Comparing in vivo approaches to assess mitochondrial function. A both unique and novel aspect of the present study was the aim to assess the relationship between four quantitative ^{31}P-MRS methods of determining mitochondrial capacity and mitochondrial respiration capacity measured in permeabilized fibers as an index of precision. Although there was some range in the strength of the relationships (r = 0.55 to 0.72), with the multipoint ADP model demonstrating the weakest relationship, each model exhibited a level of precision, as all were significantly related to State 3

respiration measured in vitro (Table 3). It is also worth noting that, although a qualitative index of mitochondrial capacity, the PCr r actually demonstrated the closest association with State 3 (r = 0.80; Fig. 3), suggestive of a greater precision with this method compared with the quantitative approaches. Although the level of precision is an important parameter when one is trying to establish the best approach to use when studying mitochondrial function in vivo, a thorough interpretation of the implications of the current results requires that the reliability and experimental conditions, which may influence this assessment, also be considered.

Both the PCr r and the peak rate of mitochondrial ATP synthesis from the linear model are influenced by the PCr content, pH, and H^+ efflux (14, 37, 56, 63), which can, in turn, negatively affect the reproducibility of these indexes (34). This shortcoming can, however, be overcome, as in the present study, by using a short exercise bout to prevent metabolic acidosis (28). In such a scenario, PCr r appears to be a good approach to qualitatively assess skeletal muscle mitochondrial capacity across individuals with a wide spectrum of activity levels. In this regard, the subjects recruited in this study exhibited a variety of physical activity levels, resulting in a large range of values for the PCr time constant (~20–70 s), consistent with the published literature in young healthy individuals [~25 s (65), ~40 s (61), 30–50 s (48), and 30–70 s (55)]. Of note, from a quantitative standpoint, the peak rate of mitochondrial ATP synthesis determined using the electrical analog model significantly overestimated muscle mitochondrial capacity (~45 mM/min; Fig. 2) and was significantly greater than the models relying on ADP as the key regulator for mitochondrial respiration. Interestingly, the calculated peak ATP synthesis determined in vitro was substantially lower than the value obtained utilizing the linear model in the present study and far below common values documented in the literature using this approach (>100 mM/min) (28, 29), further confirming that the linear method tends to overestimate the peak rate of mitochondrial ATP synthesis. This overestimation might stem from the fact that the V_{max} calculated using this approach is beyond the range of the linear approximation (PCr between 20 and 70% of total Cr) required by the electric analog model (43) and therefore would require some additional modeling of the nonlinear characteristics of the mitochondrial capacity (43). Also, although extensively

used in the literature, this approach is also questionable from a conceptual standpoint, because, in addition to the PCr r, it is dependent on resting [PCr], which has been established to be inversely proportional to the number of type I oxidative skeletal muscle fibers (24). In other words, this implies that muscle fibers with greater oxidative potential and mitochondrial volume density (type I oxidative fibers) exhibit lower [PCr], which according to the mathematical formulation of this model, would, incorrectly, translate into lower mitochondrial capacity.

The estimated V_{max} with the phosphorylation potential model was also considerably higher than the calculated ATP synthesis rate from permeabilized fiber respiration in vitro. This systematic error potentially arises from the arbitrary value set for the K_m (0.11 mM) (66), which has yet to be experimentally confirmed. In light of these issues, and considering that the reproducibility of this method has yet to be established, other methods should be preferred to quantify muscle mitochondrial capacity from ^{31}P-MRS measurements.

Although significantly higher, the ADP model provided an estimation of the peak rate of oxidative ATP synthesis that was more compatible with the currently calculated in vitro values (24 vs. 14 mM/min, $P < 0.05$) and those estimated from the literature in untrained subjects (~16–28 mM/min) (7). Interestingly, it has been documented that the peak rate of mitochondrial ATP synthesis from the kinetic ADP model is independent of pH (56) and exhibits high reproducibility (1, 34, 57). Therefore, in combination with the very good association exhibited between this index and mitochondrial respiratory capacity assessed in vitro (Fig. 3), this approach appears to provide both a precise and a reproducible measurement of mitochondrial capacity across a variety of exercise conditions. In the future, greater accuracy with this method may be achieved by directly measuring total creatine content, using, perhaps, dynamic ^{31}P-MRS in combination with ^{1}H-MRS (20).

The multipoint ADP model was the only analytical approach exhibiting both accuracy and precision compared with the in vitro measurements (Table 3; Figs. 2 and 3). However, it should be recognized that the large PCr depletion and limited pH changes induced by the exercise protocol employed in this study facilitated the analysis of the recovery period with the multipoint ADP model. Indeed, due to the need for high

time resolution, large metabolic changes, and the greater complexity of this model, unless analyses specific to the sensitivity of mitochondrial respiration to ADP are important components of a study (i.e., the K_m and Hill coefficient), the simple kinetic ADP model may, ultimately, be preferable to the multipoint ADP approach.

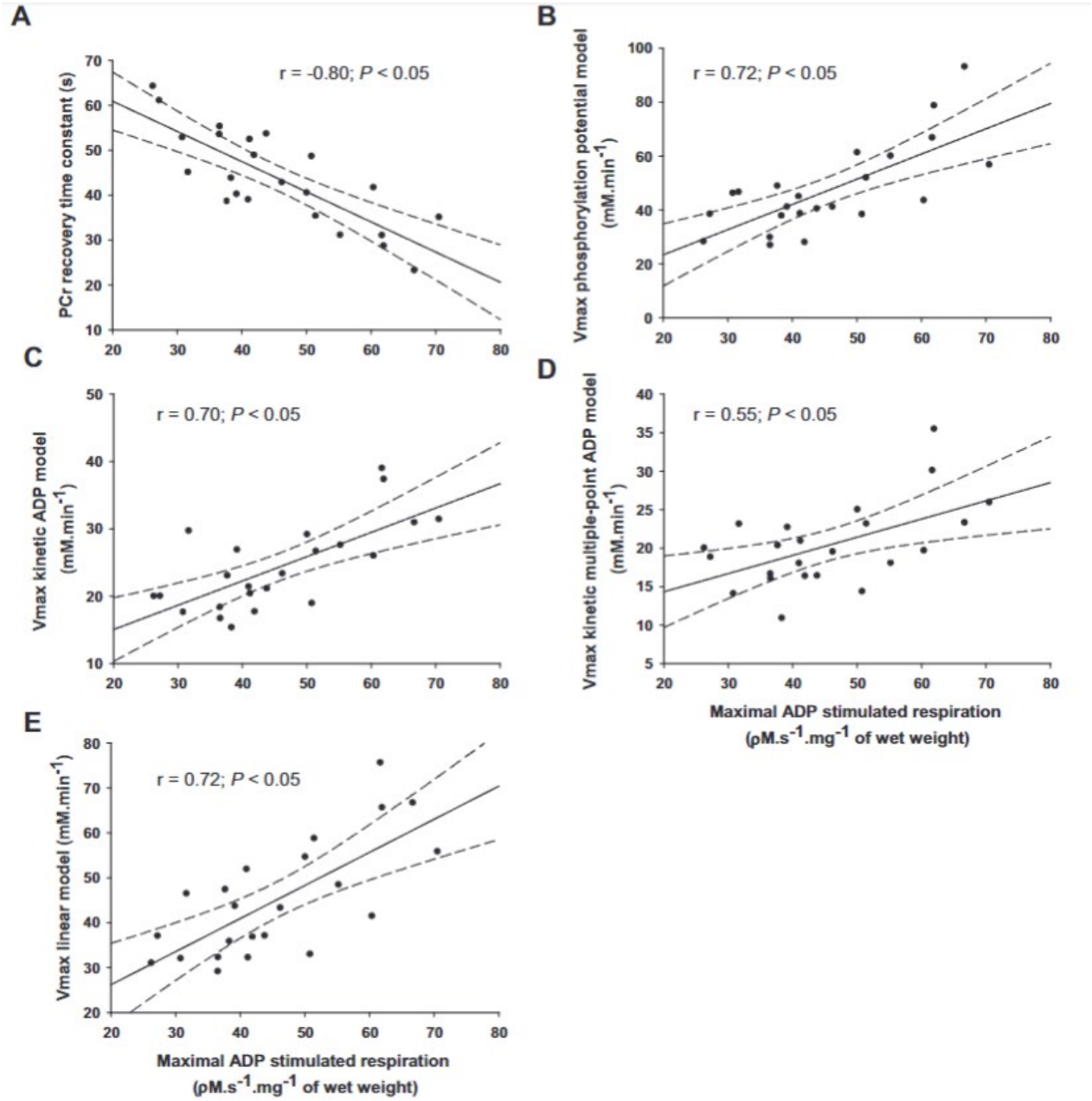

Fig. 3. Relationships between maximal ADP-stimulated respiration with convergent electron flux through Complex I and Complex II and in vivo indexes of mitochondrial capacity, i.e., the PCr recovery time constant (indirect method; *A*), the peak rate of mitochondrial ATP synthesis estimated based on a model of respiratory control by the phosphorylation potential (kinetic phosphorylation potential model; *B*), ADP using two parameters (kinetic ADP model; *C*) or multipoint analysis (multiple-point ADP model; *D*), the electrical analog model of respiratory control (linear model; *E*).

Table 3. *Summary of the positive, + and negative, - accuracy and precision findings for ^{31}P-MRS analysis approaches for assessing mitochondrial capacity in skeletal muscle*

Approach	Accuracy	Precision
PCr time constant	NA	+
Linear	–	+
ADP kinetic	–	+
ADP multipoint	+	+
Phosphorylation potential	–	+

Phosphocreatine, PCr; not applicable, NA; adenosine diphosphate, ADP.

Experimental considerations. An important aspect of the present study was to quantitatively compare the ATP synthesis rates estimated with four models in vivo and State 3 respiration measured in vitro in permeabilized skeletal muscle fibers, this latter approach being used as an external control. Although preserving most of the functional properties of the mitochondria (26, 50), it should, however, be acknowledged that this in vitro preparation still features some inherent physiological differences with the assessment of mitochondrial function by ^{31}P-MRS. This, in turn, may have resulted in some variations of the estimated rates for muscle phosphorylation capacity (Fig. 2). First, [O_2] in the respiration chamber is supraphysiological ([O_2] > 175 μM, 37°C), and the diffusion of O_2 to the mitochondria is facilitated by the permeabilization of the plasma membrane. In contrast, in vivo the intracellular O_2 partial pressure of the skeletal muscle is much lower (52, 54), and the plasma membrane is intact, potentially limiting mitochondrial ATP synthesis rate (9 –11, 36). Second, spontaneous muscle contraction (46) or collapse of the cytoskeleton (25), potentially restricting respiratory capacity, have been reported during the assessment of respiration in vitro. Third, the mechanisms of respiratory control might substantially differ in vivo and in vitro. Specifically, reducing equivalents (NADH and FADH) and ADP are all provided in saturating concentrations in vitro. On the other hand, calcium (Ca^{2+}) oscillations, which play a key role in the activation of mitochondrial respiration in vivo (22, 23), are in small and constant concentrations in the buffer solution used in vitro. Together, these differences in the regulatory parameters for oxidative phosphorylation between the two experimental approaches are likely associated with different mechanisms of metabolic control. Therefore, al- though both ^{31}P-MRS and the permeabilized fiber approach

provide a functional assessment of muscle mitochondrial properties within the environment of the muscle, it should be recognized that the conversion of respiratory rates from permeabilized fibers to in vivo conditions is subject to some inherent uncertainty.

Mitochondrial respiratory capacity was measured in vitro at a temperature of 37°C. Given the short duration of the exercise (24 s) and the thermoneutral temperature of the MR scanner (~20°C), the exercise-induced rise in muscle temperature was likely less than 0.2–0.3°C (8). Accordingly, the temperature difference between the two experimental conditions was considered negligible; therefore, the in vitro metabolic rates were not adjusted for this factor when extrapolated to in vivo conditions.

One could question the consequence on our conclusions based on the sampling of different volumes with the ^{31}P-MRS and biopsy techniques. Indeed, based on the dimension and the sensitivity of the surface coil, the MR signal originated from a much larger sample volume [vastus lateralis, vastus medialis, rectus femoris, and to a small extent from the vastus intermedius (48)] compared with the rather small muscle biopsy sample collected in the vastus lateralis (~6–10 mg). Together, the volume difference and the known variability sample to sample with the biopsy technique (39, 40) may potentially have contributed to some of the quantitative differences observed in the estimate of ATP synthesis rates in vivo and in vitro (Fig. 2). Additionally, this difference would have augmented the variance of the correlation between the respiratory capacity in vitro and the ^{31}P-MRS indexes of mitochondrial phosphorylation capacity. However, two lines of evidence suggest that our findings were not greatly confounded by this factor. First, the muscle recruitment during knee-extension exercise is homogeneous (53,) and the four muscles composing the quadriceps appear to exhibit similar metabolic properties in humans (48). Second, the four models in vivo were rather tightly correlated to the in vitro measurement of mitochondrial respiratory capacity (r = 0.55 to 0.80; Fig. 3) suggesting that the biopsy samples were representative of the quadriceps.

In addition to the consistent lack of a cytochrome *c* response during the in vitro experiments, the maximal coupled respiration with convergent electron flux through CI + CII (26–70 pM·s^{-1}·mg^{-1}) was also within the span of values previously reported in the literature [~27 pM·s^{-1}·mg^{-1} (49), 30–80 pM·s^{-1}·mg^{-1} (13), ~70 pM·s^{-1}·mg^{-1}

(30), 10–70pM·s^{-1}·mg^{-1} (45)], confirming the quality of the muscle fiber preparations.

Conclusion.

In summary, this study has revealed that each of the ^{31}P-MRS data analysis approaches, including the PCr r, provides evidence of being precise. However, only the multi- point ADP model did not overstimate the peak rate of skeletal muscle mitochondrial ATP synthesis, supportive of the conclusion that this is the only quantitative model exhibiting both accuracy and precision.

ACKNOWLEDGMENTS

We thank all the subjects in this study for their committed participation in this research.

GRANTS

This work was funded in part by grants from the Flight Attendant Medical Research Institute (FAMRI), NIH National Heart, Lung, and Blood Institute (K99 HL-125756, PO1 HL-091830), and the Veteran's Administration Rehabilitation Research and Development Service (E6910-R, E1697-R, E1433-P, and E9275-L).

DISCLOSURES

No conflicts of interest, financial or otherwise, are declared by the author(s).

AUTHOR CONTRIBUTIONS

G.L., J.R.G., J.D.T., C.R.H., Y.L.F., E.-K.J., and R.S.R. conception and design of research; G.L., J.R.G., J.D.T., C.R.H., R.S.G., S.Y.P., E.-K.J., and R.S.R. performed experiments; G.L., J.R.G., J.D.T., C.R.H., S.Y.P., and Y.L.F. analyzed data; G.L. interpreted results of experiments; G.L. prepared figures; G.L. drafted manuscript; G.L., J.R.G., J.D.T., C.R.H., Y.L.F., E.-K.J., and R.S.R. edited and revised manuscript; G.L., J.R.G., J.D.T., C.R.H., R.S.G., S.Y.P., Y.L.F., E.-K.J., and R.S.R. approved final version of manuscript.

REFERENCES

1. **Bendahan D, Mattei JP, Ghattas B, Confort-Gouny S, Le Guern ME, Cozzone PJ.** Citrulline/malate promotes aerobic energy production in human exercising muscle. *Br J Sports Med* 36: 282–289, 2002.

2. **Blomstrand E, Radegran G, Saltin B.** Maximum rate of oxygen uptake by human skeletal muscle in relation to maximal activities of enzymes in the Krebs cycle. *J Physiol* 501: 455–460, 1997.

3. **Brand MD.** The efficiency and plasticity of mitochondrial energy transduction. *Biochem Soc Trans* 33: 897–904, 2005.

4. **Chance B, Williams GR.** Respiratory enzymes in oxidative phosphorylation. I. Kinetics of oxygen utilization. *J Biol Chem* 217: 383–393, 1955.

5. **Coen PM, Jubrias SA, Distefano G, Amati F, Mackey DC, Glynn NW, Manini TM, Wohlgemuth SE, Leeuwenburgh C, Cummings SR, Newman AB, Ferrucci L, Toledo FG, Shankland E, Conley KE, Goodpaster BH.** Skeletal muscle mitochondrial energetics are associated with maximal aerobic capacity and walking speed in older adults. *J Gerontol* 68: 447–455, 2013.

6. **Forbes SC, Paganini AT, Slade JM, Towse TF, Meyer RA.** Phosphocreatine recovery kinetics following low- and high-intensity exercise in human triceps surae and rat posterior hindlimb muscles. *Am J Physiol Regul Integr Comp Physiol* 296: R161–R170, 2009.

7. **Gnaiger E.** Capacity of oxidative phosphorylation in human skeletal muscle: new perspectives of mitochondrial physiology. *Int J Biochem Cell Biol* 41: 1837–1845, 2009.

8. **Gonzalez-Alonso J, Quistorff B, Krustrup P, Bangsbo J, Saltin B.** Heat production in human skeletal muscle at the onset of intense dynamic exercise. *J Physiol 524 Pt* 2: 603–615, 2000.

9. **Haseler LJ, Hogan MC, Richardson RS.** Skeletal muscle phosphocreatine recovery in exercise-trained humans is dependent on O2 availability. *J Appl Physiol* 86: 2013–2018, 1999.

10. **Haseler LJ, Lin A, Hoff J, Richardson RS.** Oxygen availability and PCr recovery rate in untrained human calf muscle: evidence of metabolic limitation in

normoxia. *Am J Physiol Regul Integr Comp Physiol* 293: R2046 –R2051, 2007.

11. **Haseler LJ, Lin AP, Richardson RS.** Skeletal muscle oxidative metabolism in sedentary humans: 31P-MRS assessment of O2 supply and demand limitations. *J Appl Physiol* 97: 1077–1081, 2004.

12. **Hennessey JV, Chromiak JA, Della Ventura S, Guertin J, MacLean DB.** Increase in percutaneous muscle biopsy yield with a suction-enhancement technique. *J Appl Physiol (1985)* 82: 1739 –1742, 1997.

13. **Hutter E, Skovbro M, Lener B, Prats C, Rabol R, Dela F, Jansen-Durr P.** Oxidative stress and mitochondrial impairment can be separated from lipofuscin accumulation in aged human skeletal muscle. *Aging Cell* 6: 245–256, 2007.

14. **Iotti S, Lodi R, Frassineti C, Zaniol P, Barbiroli B.** In vivo assessment of mitochondrial functionality in human gastrocnemius muscle by 31P MRS. The role of pH in the evaluation of phosphocreatine and inorganic phosphate recoveries from exercise. *NMR Biomed* 6: 248 –253, 1993.

15. **Jacobs RA, Lundby C.** Mitochondria express enhanced quality as well as quantity in association with aerobic fitness across recreationally active individuals up to elite athletes. *J Appl Physiol* 114: 344 –350, 2013.

16. **Jeneson JA, Westerhoff HV, Brown TR, Van Echteld CJ, Berger R.** Quasi-linear relationship between Gibbs free energy of ATP hydrolysis and power output in human forearm muscle. *Am J Physiol Cell Physiol* 268: C1474 –C1484, 1995.

17. **Jeneson JA, Wiseman RW, Westerhoff HV, Kushmerick MJ.** The signal transduction function for oxidative phosphorylation is at least second order in ADP. *J Biol Chem* 271: 27995–27998, 1996.

18. **Jones PR, Pearson J.** Anthropometric determination of leg fat and muscle plus bone volumes in young male and female adults. *J Physiol* 204: 63P–66P, 1969.

19. **Kemp GJ, Ahmad RE, Nicolay K, Prompers JJ.** Quantification of skeletal muscle mitochondrial function by P magnetic resonance spectroscopy techniques: a quantitative review. *Acta Physiol (Oxford, UK)* 2013: 107–144, 2014.

20. **Kemp GJ, Meyerspeer M, Moser E.** Absolute quantification of phosphorus metabolite concentrations in human muscle in vivo by 31P MRS: a quantitative review. *NMR in biomedicine* 20: 555–565, 2007.

21. **Kemp GJ, Radda GK.** Quantitative interpretation of bioenergetic data from 31P and 1H magnetic resonance spectroscopic studies of skeletal muscle: an analytical review. *Magn Reson Q* 10: 43–63, 1994.

22. **Korzeniewski B.** “Idealized” state 4 and state 3 in mitochondria vs. rest and work in skeletal muscle. *PloS One* 10: e0117145, 2015.

23. **Korzeniewski B, Rossiter HB.** Each-step activation of oxidative phosphorylation is necessary to explain muscle metabolic kinetic responses to exercise and recovery in humans. *J Physiol* 593: 5255–5268, 2015.

24. **Kushmerick MJ, Moerland TS, Wiseman RW.** Mammalian skeletal muscle fibers distinguished by contents of phosphocreatine, ATP, and Pi. *Proc Natl Acad Sci USA* 89: 7521–7525, 1992.

25. **Kuznetsov AV, Guzun R, Boucher F, Bagur R, Kaambre T, Saks V.** Mysterious Ca(2+)-independent muscular contraction: deja vu. *Biochem J* 445: 333–336, 2012.

26. **Kuznetsov AV, Veksler V, Gellerich FN, Saks V, Margreiter R, Kunz WS.** Analysis of mitochondrial function in situ in permeabilized muscle fibers, tissues and cells. *Nat Protocols* 3: 965–976, 2008.

27. **Lanza IR, Befroy DE, Kent-Braun JA.** Age-related changes in ATP-producing pathways in human skeletal muscle in vivo. *J Appl Physiol* 99: 1736 –1744, 2005.

28. **Lanza IR, Bhagra S, Nair KS, Port JD.** Measurement of human skeletal muscle oxidative capacity by 31P-MR spectroscopy: a cross-validation with in vitro measurements. *J Magn Reson Imaging* 34: 1143–1150, 2011.

29. **Larsen RG, Callahan DM, Foulis SA, Kent-Braun JA.** In vivo oxidative capacity varies with muscle and training status in young adults. *J Appl Physiol* 107: 873–879, 2009.

30. **Larsen S, Hey-Mogensen M, Rabol R, Stride N, Helge JW, Dela F.** The influence of age and aerobic fitness: effects on mitochondrial respiration in skeletal muscle. *Acta Physiol (Oxford, UK)* 205: 423–432, 2012.

31. **Larsen S, Nielsen J, Hansen CN, Nielsen LB, Wibrand F, Stride N, Schroder HD, Boushel R, Helge JW, Dela F, Hey-Mogensen M.** Biomarkers of

mitochondrial content in skeletal muscle of healthy young human subjects. *J Physiol* 590: 3349–3360, 2012.

32. **Larson-Meyer DE, Newcomer BR, Hunter GR, Joanisse DR, Weinsier RL, Bamman MM.** Relation between in vivo and in vitro measurements of skeletal muscle oxidative metabolism. *Muscle Nerve* 24: 1665–1676, 2001.

33. **Layec G, Bringard A, Le Fur Y, Vilmen C, Micallef JP, Perrey S, Cozzone PJ, Bendahan D.** Comparative determination of energy production rates and mitochondrial function using different (31) P MRS quantitative methods in sedentary and trained subjects. *NMR Biomed* 24: 425–438, 2011.

34. **Layec G, Bringard A, Le Fur Y, Vilmen C, Micallef JP, Perrey S, Cozzone PJ, Bendahan D.** Reproducibility assessment of metabolic variables characterizing muscle energetics in vivo: A 31P-MRS study. *Magn Reson Med* 62: 840–854, 2009.

35. **Layec G, Haseler LJ, Hoff J, Hart CR, Liu X, Le Fur Y, Jeong EK, Richardson RS.** Short-term training alters the control of mitochondrial respiration rate before maximal oxidative ATP synthesis. *Acta Physiol (Oxford, UK)* 208: 376–386, 2013.

36. **Layec G, Haseler LJ, Trinity JD, Hart CR, Liu X, Le Fur Y, Jeong EK, Richardson RS.** Mitochondrial function and increased convective O2 transport: implications for the assessment of mitochondrial respiration in vivo. *J Appl Physiol (1985)* 115: 803–811, 2013.

37. **Layec G, Malucelli E, Le Fur Y, Manners D, Yashiro K, Testa C, Cozzone PJ, Iotti S, Bendahan D.** Effects of exercise-induced intracellular acidosis on the phosphocreatine recovery kinetics: a 31P MRS study in three muscle groups in humans. *NMR Biomed* 26: 1403–1411, 2013.

38. **Le Fur Y, Nicoli F, Guye M, Confort-Gouny S, Cozzone PJ, Kober F.** Grid-free interactive and automated data processing for MR chemical shift imaging data. *Magma (New York)* 23: 23–30, 2010.

39. **Lexell J, Henriksson-Larsen K, Sjostrom M.** Distribution of different fibre types in human skeletal muscles. 2. A study of cross-sections of whole m. vastus lateralis. *Acta Physiol Scand* 117: 115–122, 1983.

40. **Lexell J, Taylor CC.** Variability in muscle fibre areas in whole human quadriceps muscle. How much and why? *Acta Physiol Scand* 136: 561– 568, 1989.

41. **Mahler M.** First-order kinetics of muscle oxygen consumption, and an equivalent proportionality between QO2 and phosphorylcreatine level. Implications for the control of respiration. *J Gen Physiol* 86: 135–165, 1985.

42. **McCully KK, Fielding RA, Evans WJ, Leigh JS Jr, Posner JD.** Relationships between in vivo and in vitro measurements of metabolism in young and old human calf muscles. *J Appl Physiol* 75: 813–819, 1993.

43. **Meyer RA.** A linear model of muscle respiration explains monoexponential phosphocreatine changes. *Am J Physiol Cell Physiol* 254: C548 –C553, 1988.

44. **Paganini AT, Foley JM, Meyer RA.** Linear dependence of muscle phosphocreatine kinetics on oxidative capacity. *Am J Physiol Cell Physiol* 272: C501–C510, 1997.

45. **Park SY, Gifford JR, Andtbacka RH, Trinity JD, Hyngstrom JR, Garten RS, Diakos NA, Ives SJ, Dela F, Larsen S, Drakos S, Richardson RS.** Cardiac, skeletal, and smooth muscle mitochondrial respiration: are all mitochondria created equal? *Am J Physiol Heart Circ Physiol* 307: H346 –H352, 2014.

46. **Perry CG, Kane DA, Lin CT, Kozy R, Cathey BL, Lark DS, Kane CL, Brophy PM, Gavin TP, Anderson EJ, Neufer PD.** Inhibiting myosin- ATPase reveals a dynamic range of mitochondrial respiratory control in skeletal muscle. *Biochem J* 437: 215–222, 2011.

47. **Pesta D, Gnaiger E.** High-resolution respirometry: OXPHOS protocols for human cells and permeabilized fibers from small biopsies of human muscle. *Methods Mol Biol (Clifton, NJ)* 810: 25–58, 2012.

48. **Pesta D, Paschke V, Hoppel F, Kobel C, Kremser C, Esterhammer R, Burtscher M, Kemp GJ, Schocke M.** Different metabolic responses during incremental exercise assessed by localized 31P MRS in sprint and endurance athletes and untrained individuals. *Int J Sports Med* 34: 669 – 675, 2013.

49. **Phielix E, Schrauwen-Hinderling VB, Mensink M, Lenaers E, Meex R, Hoeks J, Kooi ME, Moonen-Kornips E, Sels JP, Hesselink MK, Schrauwen P.** Lower intrinsic ADP-stimulated mitochondrial respiration underlies in vivo mitochondrial

dysfunction in muscle of male type 2 diabetic patients. *Diabetes* 57: 2943–2949, 2008.

50. **Picard M, Taivassalo T, Ritchie D, Wright KJ, Thomas MM, Romestaing C, Hepple RT.** Mitochondrial structure and function are disrupted by standard isolation methods. *PloS One* 6: e18317, 2011.

51. **Quistorff B, Johansen L, Sahlin K.** Absence of phosphocreatine resynthesis in human calf muscle during ischaemic recovery. *Biochem J* 291: 681–686, 1993.

52. **Richardson RS, Duteil S, Wary C, Wray DW, Hoff J, Carlier PG.** Human skeletal muscle intracellular oxygenation: the impact of ambient oxygen availability. *J Physiol* 571: 415–424, 2006.

53. **Richardson RS, Frank LR, Haseler LJ.** Dynamic knee-extensor and cycle exercise: functional MRI of muscular activity. *Int J Sports Med* 19: 182–187, 1998.

54. **Richardson RS, Knight DR, Poole DC, Kurdak SS, Hogan MC, Grassi B, Wagner PD.** Determinants of maximal exercise VO2 during single leg knee-extensor exercise in humans. *Am J Physiol Heart Circ Physiol* 268: H1453–H1461, 1995.

55. **Rossiter HB, Ward SA, Kowalchuk JM, Howe FA, Griffiths JR, Whipp BJ.** Dynamic asymmetry of phosphocreatine concentration and O(2) uptake between the on- and off-transients of moderate- and high- intensity exercise in humans. *J Physiol* 541: 991–1002, 2002.

56. **Roussel M, Bendahan D, Mattei JP, Le Fur Y, Cozzone PJ.** 31P magnetic resonance spectroscopy study of phosphocreatine recovery kinetics in skeletal muscle: the issue of intersubject variability. *Biochim Biophys Acta* 1457: 18 – 26, 2000.

57. **Sedivy P, Christina Kipfelsberger M, Dezortova M, Krssak M, Drobny M, Chmelik M, Rydlo J, Trattnig S, Hajek M, Valkovic L.** Dynamic (31)P MR spectroscopy of plantar flexion: Influence of ergometer design, magnetic field strength (3 and 7 T), and RF-coil design. *Med Physics* 42: 1678, 2015.

58. **Taylor DJ, Bore PJ, Styles P, Gadian DG, Radda GK.** Bioenergetics of intact human muscle. A 31P nuclear magnetic resonance study. *Mol Biol Med* 1: 77–94, 1983.

59. **Thompson CH, Kemp GJ, Sanderson AL, Radda GK.** Skeletal muscle

mitochondrial function studied by kinetic analysis of postexercise phosphocreatine resynthesis. *J Appl Physiol* 78: 2131–2139, 1995.

60. **Trenell MI, Sue CM, Kemp GJ, Sachinwalla T, Thompson CH.** Aerobic exercise and muscle metabolism in patients with mitochondrial myopathy. *Muscle Nerve* 33: 524 –531, 2006.

61. **Valkovic L, Ukropcova B, Chmelik M, Balaz M, Bogner W, Schmid AI, Frollo I, Zemkova E, Klimes I, Ukropec J, Trattnig S, Krssak M.** Interrelation of 31P-MRS metabolism measurements in resting and exercised quadriceps muscle of overweight-to-obese sedentary individuals. *NMR Biomed* 26: 1714 –1722, 2013.

62. **van den Broek NM, Ciapaite J, Nicolay K, Prompers JJ.** Comparison of in vivo postexercise phosphocreatine recovery and resting ATP syn- thesis flux for the assessment of skeletal muscle mitochondrial function. *Am J Physiol Cell Physiol* 299: C1136 –C1143, 2010.

63. **van den Broek NM, De Feyter HM, de Graaf L, Nicolay K, Prompers JJ.** Intersubject differences in the effect of acidosis on phosphocreatine recovery kinetics in muscle after exercise are due to differences in proton efflux rates. *Am J Physiol Cell Physiol* 293: C228 –C237, 2007.

64. **Vanhamme L, van den Boogaart A, Van Huffel S.** Improved method for accurate and efficient quantification of MRS data with use of prior knowledge. *J Magn Reson* 129: 35–43, 1997.

65. **Vanhatalo A, Fulford J, Bailey SJ, Blackwell JR, Winyard PG, Jones AM.** Dietary nitrate reduces muscle metabolic perturbation and improves exercise tolerance in hypoxia. *J Physiol* 589: 5517–5528, 2011.

66. **Walter G, Vandenborne K, Elliott M, Leigh JS.** In vivo ATP synthesis rates in single human muscles during high intensity exercise. *J Physiol* 519: 901–910, 1999.

67. **Wüst RC, Grassi B, Hogan MC, Howlett RA, Gladden LB, Rossiter HB.** Kinetic control of oxygen consumption during contractions in self- perfused skeletal muscle. *J Physiol* 589: 3995–4009, 2011.